energies

MDPI

Article

# Boiling Synchronization in Two Parallel Minichannels—Image Analysis

**Gabriela Rafałko, Iwona Zaborowska *, Hubert Grzybowski and Romuald Mosdorf**

Department of Mechanics and Applied Computer Science, Faculty of Mechanical Engineering Bialystok University of Technology, Wiejska 45 C, 15-351 Bialystok, Poland; rafalkogabriela@gmail.com (G.R.); h.grzybowski@pb.edu.pl (H.G.); r.mosdorf@pb.edu.pl (R.M.)

* Correspondence: iwonag94@wp.pl

Received: 15 December 2019; Accepted: 3 March 2020; Published: 18 March 2020


**Abstract:** In this paper, the boiling synchronization of two-phase flow patterns in two parallel minichannels of 1 mm in diameter with connected compressible volumes was analyzed. The analysis was performed using images recorded with a high-speed camera. The degree of synchronization between channels was evaluated by assessing the presence of liquid flow in the small part of the minichannels. It can be concluded that boiling is synchronized when small bubble flow or wavy annular flow occur in neighboring channels. The occurrence of slug flow in one channel causes the boiling in neighboring channels to become unsynchronized. The result of the image analysis shows that the correlation coefficient based on the evaluation of the presence of liquid flow in the small part of the minichannels over a long enough time period allows for the detection of boiling synchronization.

**Keywords:** two-phase flow instability; image analysis; flow pattern; flow boiling; boiling synchronization

## 1. Introduction

The continuous formation of different flow patterns that change during two-phase flow with boiling leads to the occurrence of numerous instabilities. Instabilities in minichannels such as heat transfer, pressure drop, and flow pattern oscillations were deeply investigated [1–3]. In many cases, several instabilities happen simultaneously in the system [4]. This occurs when instability of one type causes an oscillation that is overlapped by another oscillation caused by a different instability. Due to such a phenomenon, different types of flows were observed [5]. In the literature, instabilities were specified not only as flow instabilities but also as parallel channel instabilities. In the paper [6], authors investigated two types of fluctuations in parallel channels: one where the oscillations in the channels were in phase, and the other where the oscillations behaved chaotically. What is more, in two-phase flow with phase change, which is an example of a nonlinear process, synchronization oscillations may occur according to the authors of the paper [7].

The challenge considering the identification and description of boiling synchronization in a flow includes choosing an appropriate method for the stated task. Already, numerous approaches have been taken in order to analyze two-phase flow, such as nonlinear analysis [5,8,9], Eulerian space–time correlations [10], modeling [11,12], and image analysis [10,13,14]. The method mentioned last is based on processing frames registered by, for example, a high-speed camera, which presents a real-time image of the observed flow. Using image analysis, one can assess the size of the flow's particles or their displacement [13]. What is more, image processing may give information about the dynamic character of the flow [14]. In the field of image analysis, coefficients or thresholds are often introduced in order to classify the observed flow patterns [1,15].

In this paper, the synchronization of boiling in two parallel minichannels was determined using image analysis. The degree of synchronization between channels was evaluated by assessing the presence of liquid flow in the small part of the minichannels over a long time period.

The experimental setup and image data analysis are presented in Section 2. Section 3 describes the results and discussion. The conclusion of this paper is included in Section 4.

## 2. Materials and Methods

A schematic diagram of the experimental setup is shown in Figure 1. The main element of the system was a set of two parallel minichannels (1, 2—Figure 1) in which the boiling process took place. The distilled water was given by a pressure-driven subsystem, which consisted of an air compressor and a precision proportional pressure regulator that maintained constant overpressure in the supply tank (3—Figure 1). A flow control valve (5—Figure 1) was used to regulate the water flow rate. The Coriolis mass flow meter (4—Figure 1), with ± 0.2% accuracy, was used for monitoring the flow. Each channel had its separate surge tank (6, 7—Figure 1), which could be treated as a compressible volume. Water from each surge tank flowed into a circular brass pipe (1, 2—Figure 1) with an inner diameter of 1, an outer diameter of 2, and a length of 150 mm. Channels were placed in the isolated heating section, which was heated by Kanthal heating elements. The thermocouples (type K with a diameter of 0.081 mm and ± 0.8 °C accuracy, response time approx. 0.025 s) were placed with a distance of 5 mm from the heated part of the channel's outlet. They measured the temperature of the brass channel wall. The glass tube (length of 150, an inner diameter of 1, and an outer diameter of 5.7 mm) was attached to the end of each channel and allowed the recording of flow patterns. Images were captured using a Phantom v1610 (8—Figure 1) high-speed camera at 300 fps. The content of the channel was also qualitatively assessed using a laser-phototransistor sensor (10—Figure 1). Inlet and outlet pressure in each brass pipe was measured using the silicon pressure sensor MPX5010DP (range 0–50 kPa, sensitivity 1.2 mV/kPa, response time 1 ms, accuracy ± 1.25 kPa). Data from sensors were acquired using the data acquisition system (Data translation 9805, an accuracy of 1 mV for voltages in the range of −10 V to 10 V) at a sampling rate of 1 kHz. Condensed water went into the overflow tank from the minichannels (9—Figure 1).

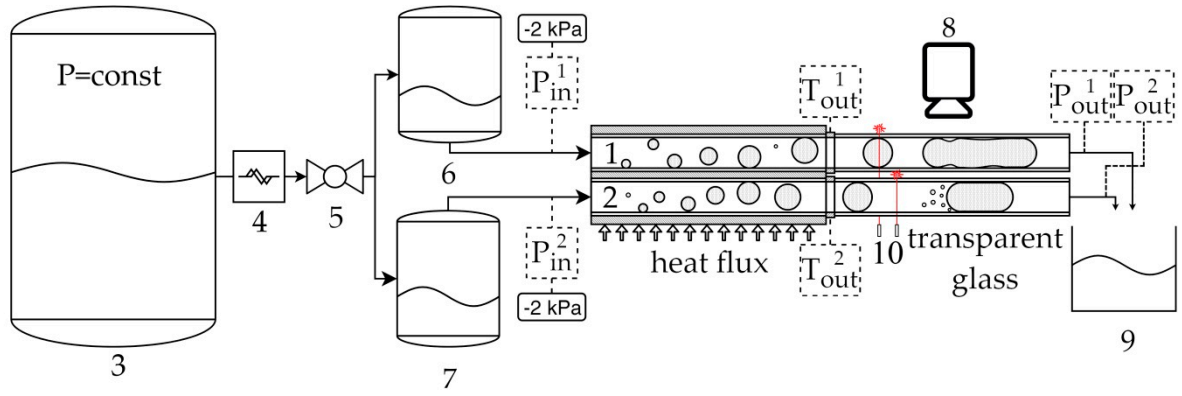


**Figure 1.** Schematic diagram of the experimental setup: 1, 2—minichannels; 3—supply tank with constant overpressure; 4—Coriolis mass flow meter; 5—ball valve; 6, 7—surge tanks; 8—high-speed camera; 9—overflow tank; 10—laser–phototransistor sensors.

### 2.1. Test Conditions and Procedures

Table 1 shows the experiment conditions for the data that were analyzed in this paper. The experiment for parallel channels was carried out under a constant amount of heat generated by heaters at 55.8 W. The average mass flux $G$ was computed from the value recorded by the flow meter divided by the cross-sectional area of both channels. Thus, the average mass flux was equal to 38.8 kg/m$^2$s and oscillated in the range of ± 0.5 kg/m$^2$s due to long periodic pressure drop oscillations.

**Table 1.** The conditions of the experiment.

| Parameter | Value | Unit | Accuracy |
|---|---|---|---|
| Average mass flux $G$ | 38.8 | kg/m$^2$s | ±1 |
| Heat input $P$ | 55.8 | W | ±0.02 |
| Overpressure in supply tank | 15.0 | MPa | ±0.1 |
| Room temperature | 19.6 | °C | ±0.5 |

The pressure in the inlet and outlet of each channel was measured with a silicon pressure sensor with a response time of 0.001 s. The sensors were located near the inlet and the outlet of the minichannels. In the recent experiment, the oscillations caused by one type of instability were superimposed on another type, leading to chaotic pressure oscillations. Figure 2 shows a reference case for the superimposed density wave oscillations during pressure drop oscillations in each channel. This phenomenon was observed for heat input exceeding 50 W. Similar kinds of oscillations were reported in other papers [2,3]. Long-period (approx. 300 s) oscillations associated with the presence of compressible volumes in the tested system were observed. This observation was confirmed by other researchers [4,5]. Additionally, short-period density wave oscillations were superimposed on long-period pressure drop oscillations. The single cycle from which image data were analyzed is denoted by a rectangle in Figure 2a as the single cycle. The average values of the pressure drop oscillations are marked with a white line. Single cycle of inlet pressure, void fraction of two-phase flow, and wall temperature times series for both minichannels are included in Figure 2b–d.

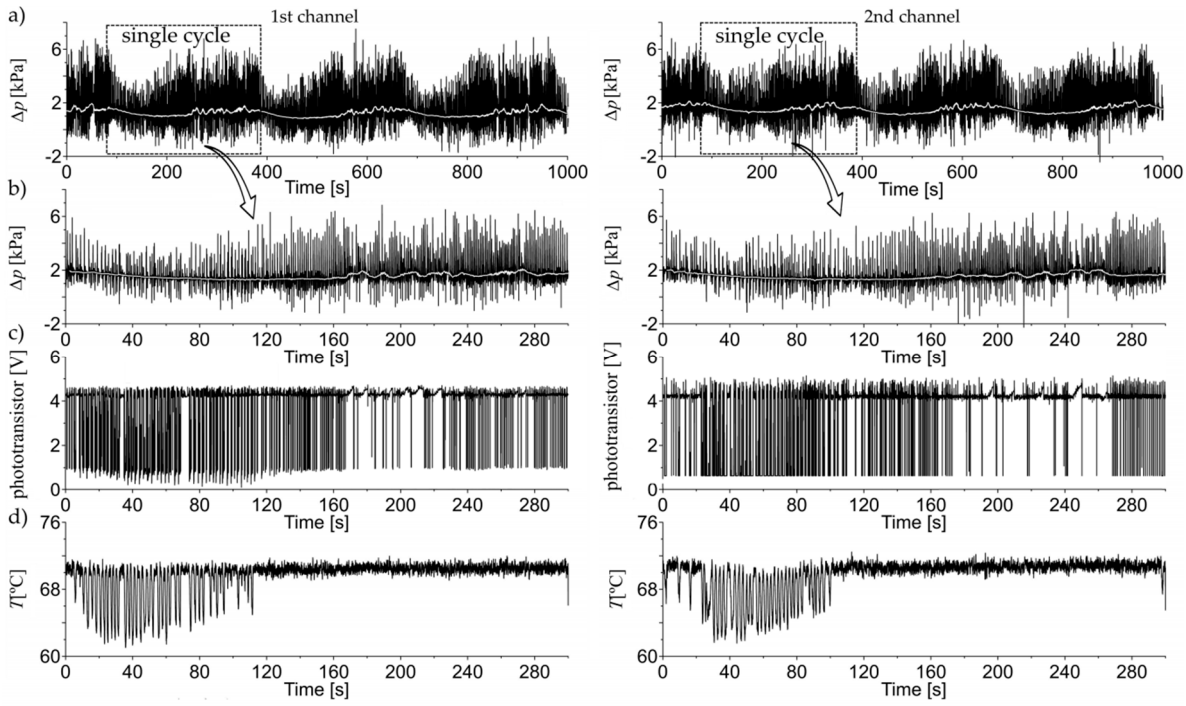


**Figure 2.** The experimental data at $G$ = 38.8 kg/m$^2$s and $P$ = 55.8 W: (**a**) pressure drop oscillation (entire signal); (**b**) pressure drop oscillation in single cycle; (**c**) void fraction of two-phase flow; (**d**) outlet channel wall temperature.

The data presented in Figure 2a,b were recorded by inlet pressure sensor, but because the system under consideration was an open loop type, it was assumed that the outlet pressure was equal to the atmospheric pressure. Inlet pressure sensor was a differential type. The condensation process occurring in the channels generated the underpressure; thus, in order to record such pressure fluctuations, the second port of the inlet pressure sensor was connected to the chamber with underpressure equal to −2kPa. Finally, the $\Delta p$ presented in Figure 2 is equal to $p_{in} - p_{atm}$.

The conditions for both analyzed channels are not the same, which was caused by small differences in the quality of both channels' heating surfaces, as well as slight differences in the channels' heating and their geometry. Nevertheless, in our opinion, these slight differences do not have a significant impact on the character of pressure interactions between channels. The temperature changes are the result of changes in the flow pattern in the channels and occur with a lower frequency than pressure fluctuations. This is caused by the thermal inertia of the heating system. Pressure changes occurring in a short period of time are associated with the formation or disappearance of individual steam slugs in the channels. Therefore, when pressure changes are recorded with a sufficiently high frequency, we observe pressure fluctuations as shown in Figure 2. Decreasing the recording frequency smooths the function of pressure changes (this curve is marked with a white line in Figure 2).

During flow boiling instability, different flow patterns were observed. Example frames with characteristic flow patterns are shown in Figure 3. Local pressure in the heated part of the channel fluctuated due to the boiling. These pressure oscillations led to the acceleration of the two-phase mixture. Thus, the observed flow patterns shown in Figure 3 were mainly bubble, slug, confident slug, or wavy annular flow, and their flow velocities varied.

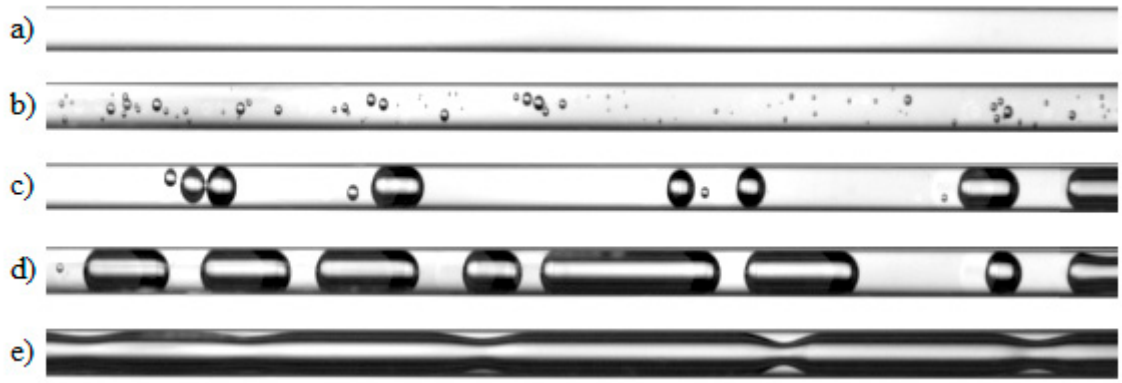


**Figure 3.** Recorded frames with characteristic flow patterns: (**a**) liquid flow; (**b**) small bubble flow; (**c**) bubble flow; (**d**) slug flow; (**e**) wavy annular flow.

### 2.2. Detecting the Presence of Water Using Image Analysis

The images recorded with a high-speed camera with a frequency of 300 fps were used to determine the changes in time of the presence of liquid flow (Figure 3a) in a part of the minichannel that was 0.57 mm long (4 pixels). Such length was limited by the frame resolution and the size of the small bubbles. Two sets of subsequent frames (Figure 4a), which were extracted from the video, were processed. The sets of the frames were represented by matrices of grayscale pixels (21 × 1103 pixels). The parts of the frame (gates—21 × 4 pixels) located at the beginning of a frame were analyzed. The gate located in the first minichannel (Figure 1) was denoted as $G^1$ and the gate located in the second minichannel was denoted as $G^2$ (Figure 4a). The gates were located at the beginning of the transparent glass channel's section where the results of processes occurring in the heated section could be observed.

The presence of water in the gates was evaluated by a sum, $S$, of the gates' pixels' brightness. The following time series were defined:

$$S_1(t) = \sum\nolimits_{i,j} G^1_{i,j}(t) \quad (1)$$

$$S_2(t) = \sum\nolimits_{i,j} G^2_{i,j}(t) \quad (2)$$

where $G^1_{i,j}(t)$ and $G^2_{i,j}(t)$ denote the pixel brightness in gate $G^1$ and $G^2$ at the moment of time $t$. The indexes $i$ and $j$ denote the pixels' position in the gates.

The value of the threshold, $\varepsilon$, defining the liquid presence in the gates depended on the lighting condition. The threshold was set on the basis of video analysis and it was $\varepsilon$ = 12,000. A value greater than 12,000 indicated the presence of only water in the gate. The following time series were defined:

$$L_1(t) = \Theta[\varepsilon - S_1(t)] \tag{3}$$

$$L_2(t) = \Theta[\varepsilon - S_2(t)] \tag{4}$$

where $\Theta$ is a Heaviside function.

The percentage presence of liquid flow in two-phase flow over a particular time period ($\xi$) was calculated. The following time series were defined:

$$SL_1(t) = \frac{1}{\xi}\sum_t^{t+\xi} L_1 \tag{5}$$

$$SL_2(t) = \frac{1}{\xi}\sum_t^{t+\xi} L_2 \tag{6}$$

Image analysis was performed using MATLAB software R2014. The graph (Figure 4c) shows the example of changes in time of the sum of gate pixel brightness.

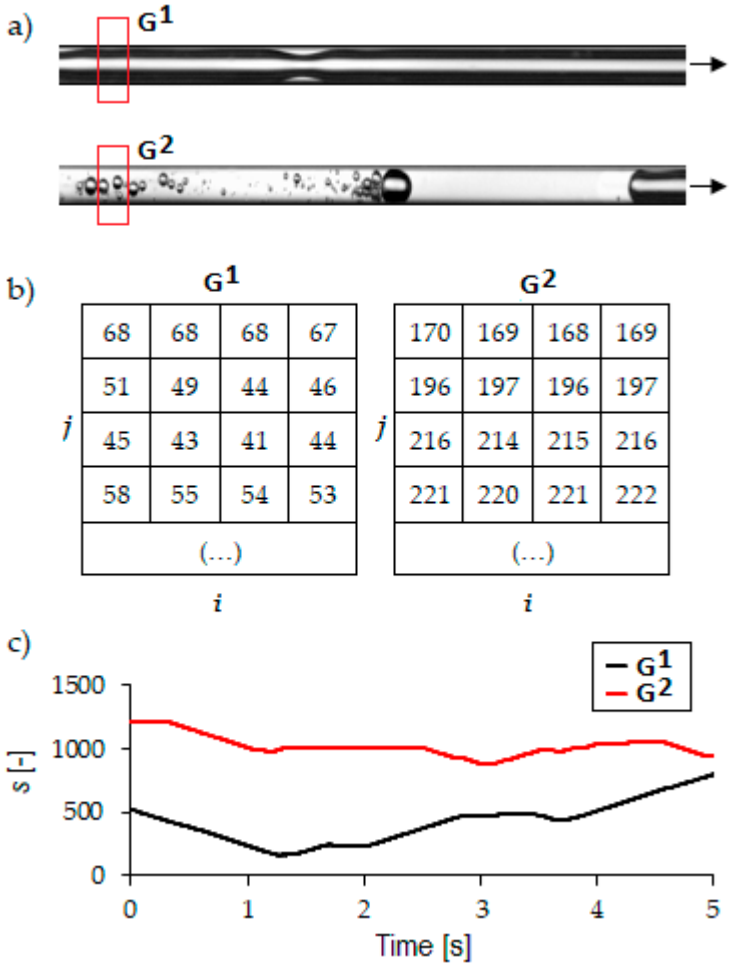


**Figure 4.** The two-phase flow pattern recognition algorithm: (**a**) sample frames with flow patterns recorded for two minichannels. The images were taken in the 65.342 second of the pressure drop cycle; (**b**) the matrices of grayscale pixels for two selected frames for t = 0 s. The sum of brightness pixels for $G^1$ is equal to 510, while the sum of brightness pixels for $G^2$ is equal to 1230; (**c**) the level of liquid flow presence in the two-phase flow in two parallel minichannels.

The correlation analysis of these signals (Figure 2c) does not give positive results. In our opinion, this is due to the light reflections from the bubbles' surface and light deflections caused by the shape of the bubbles. Therefore, the image analysis was performed for a precisely defined region of analysis in which a threshold assessment was used. Only two states in the channels were identified: liquid flow and flow with steam (different bubble size).

The two-phase flows observed in the minichannels consisted of small and large bubbles, short and long slugs, and steam. In the boiling process, also due to the pressure interactions between the channels, the flow patterns in the neighboring channels changed rapidly. Changes occurring in each moment of time made it impossible to assess the degree of the flows' synchronization in the channels. In order to estimate the degree of the synchronization of the phenomena in the neighboring minichannels, the correlation coefficient in the moving window of length, $\tau$, was calculated. The correlation coefficient is defined as follows:

$$r = \frac{\sum_t^{t+\tau} (L_1 - \overline{L}_1)(L_2 - \overline{L}_2)}{\sigma(L_1)\sigma(L_2)} \quad (7)$$

where σ is a standard deviation respectively of $L_1$ and $L_2$. $\overline{L}_1$ and $\overline{L}_2$ are mean values of $L$ in time period $\tau$.

The $r$ value is related to the occurrence of liquid flow in the minichannels. When the value of $r$ was close to 1, then at the same moment in time, the liquid flow appeared in both channels simultaneously. When the value of $r$ was close to 0, the appearance of liquid flow in both channels was not correlated. When the value of $r$ was less than 0, the appearance of liquid flow in channels was correlated, but at the same moment in time, liquid flow appeared only in one channel.

Therefore, in order to assess the degree of synchronization of phenomena occurring in channels, the presence of water in a longer period of time should be considered. The percentage presence of liquid flow in two-phase flow in different time periods, $\xi$, equal to 1.6, 3.3, and 5 s, was analyzed. Next, the correlation coefficient of changes in the percentage presence of liquid flow in two-phase flow was estimated in the time period $\tau$ = 6.7 s.

As a result of the changes in the two-phase flow patterns, the correlation coefficient values oscillated (Figure 5a), which made it difficult to assess the degree of boiling synchronization over a long period of time. In order to assess the tendency of changes in the correlation coefficient over a long period of time, the obtained results were smoothed using a moving average method in the 10 s interval (Figure 5b).

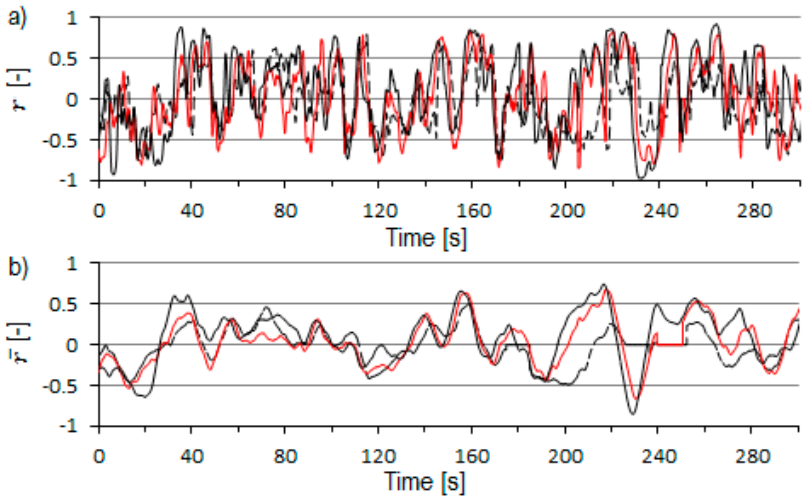


**Figure 5.** Correlation coefficient of changes in the percentage presence of liquid flow in two-phase flow: (**a**) black line—the presence of liquid flow in 1.6 s, pointed black line—the presence of liquid flow in 3.3 s, and red line—the presence of liquid flow in 5 s; (**b**) the smoothed function of $r$ (in moving window: 10 s).

## 3. Results and Discussion

The images recorded with a high-speed camera in each parallel minichannel were processed using image analysis. Figure 6a,b shows the pressure drop oscillations of two neighboring minichannels. Figure 6c presents the results of the image analysis indicating the function *SL* (Equations (5) and (6)).

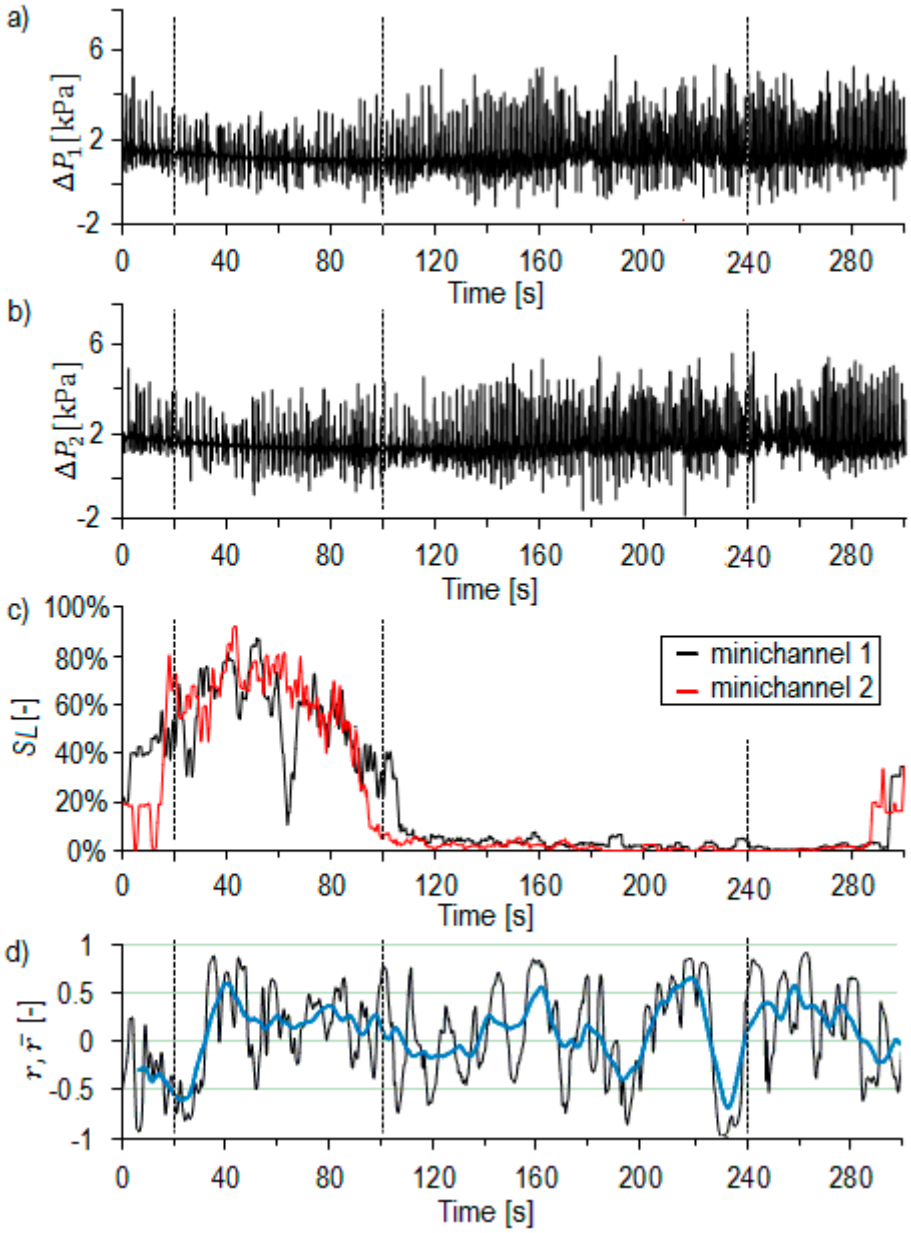


**Figure 6.** The obtained results of image analysis: (**a**) the pressure drop oscillations in the first minichannel; (**b**) the pressure drop oscillations in the second minichannel; (**c**) the percentage presence of liquid flow in two-phase flow in a 5 s time period; (**d**) the correlation coefficients specifying the degree of synchronization in two parallel minichannels. The blue line indicates changes in the percentage presence of liquid flow in 10 s, whereas the black line in 5 s.

At a value close to 100%, the minichannels were filled with water, while at a value of about 0, wavy annular flow appeared in the minichannels. Intermediate values mean that in addition to water flow in the channel, other flow patterns were observed. In Figure 6d, the smoothed function of $r$ (in moving window: 10 s—blue line) and the correlation coefficient of changes in the percentage presence of liquid flow in 5 s (black line) are presented.

The analyzed process of boiling was divided into four time periods. At the beginning of the process, in the time period 0–20 s, the value of $r$ was less than 0. In one of the channels liquid flow occurred, whereas in the second channel slug flow was observed.

In time period 20–100 s, a large value of the $SL$ coefficient indicated the presence of a relatively large amount of liquid flow in the minichannels. In this period of time, bubble flow in the channels was observed. For such a flow, the smoothed function of $r$ was positive. It indicated that the boiling processes occurring in neighboring channels were synchronized—mostly (on average) at the same time that the same flow patterns in the channels were observed.

In time period 100–240 s, the value of the $SL$ coefficient indicated the presence of a relatively small amount of liquid flow in the minichannels. The process of boiling was rapid—in both channels, slug flow, wavy annular flow, and bubble flow were observed. The smoothed function of $r$ oscillated. This happened as a result of the occurrence of slug flow during wavy annular flow. An increase or decrease in the value of $r$ meant that flow patterns in neighboring channels were unsynchronized. Mostly (on average), different flow patterns occurred at the same time in both channels.

In time period 240–290 s, the value of the $SL$ coefficient indicated the presence of a relatively small amount of liquid flow in the minichannels. The smoothed function of $r$ was greater than 0. This was because the channels were filled with wavy annular flow, which indicated that the boiling processes occurring in neighboring channels were synchronized. The synchronized wavy annular flow became less intense at 280 s and the smoothed function of $r$ decreased—a new cycle of boiling (shown in Figure 1) was started.

The difference in the brightness of the pixels corresponding to the presence of water or vapor in the channel was significant; therefore, small changes in the threshold value caused a small change in the amount of detected water in the channel. For example, a 20% change in the threshold value (from 12,000 to 10,000) caused the total number of detected water flow to change by 2.08%. However, the average correlation between signals changed by 4.01%.

## 4. Conclusions

In this paper, the analysis of images recorded using a high-speed camera for two parallel minichannels with a diameter of 1 mm was presented. Non-stationary boiling was observed in the system due to the presence of long-time pressure oscillations related to the presence of compressible volumes in the system. The individual compressible volumes were connected: What caused the pressure to drop in one channel influenced pressure changes in the second channel.

The degree of synchronization between boiling in the channels was evaluated by assessing the presence of the liquid flow in the small part of the minichannels. The correlation coefficient based on evaluating the presence of the liquid flow in a small part of minichannels over a long-enough time period was used to determine boiling synchronization in neighboring channels.

We can conclude that boiling is synchronized when small bubble flow or wavy annular flow occurs in neighboring channels. The occurrence of slug flow in one channel causes boiling to become unsynchronized. This is related to the pressure interactions between compressible volumes.

From previous papers [16,17], we know that the appearance of unending oscillations of the void fraction with a different frequency is determined by the compressible volume in the system and the type of two-phase flow patterns in the minichannel. In the considered system, the compressible volumes are the volumes of the tanks (Figure 1—6, 7) filled with air. In both tanks, the air pressure was the same. Changes in the compressible volume connected to one channel do not directly change the second compressible volume. Such a process only slightly modifies the air pressure in both tanks.

Therefore, we can suppose that in the considered system the synchronization between processes occurring in channels happens by changing the dominant frequency of void fraction changes in neighboring channels. When we consider the system with the connection of inlets of channels, then the above-mentioned mechanism is supplemented by the process of changing the inlet liquid temperature—the liquid temperature is modified by reverse flows.

**Author Contributions:** Conceptualization, G.R., I.Z., H.G., and R.M.; data curation, H.G. and R.M.; formal analysis, G.R., I.Z., H.G., and R.M.; funding acquisition; investigation, H.G.; methodology, G.R., I.Z., H.G., and R.M.; project administration, H.G. and R.M.; resources, H.G.; supervision, R.M.; validation, G.R. and R.M.; visualization, G.R., I.Z., H.G., and R.M.; writing—original draft, I.Z. and R.M.; writing—review and editing, G.R., I.Z, H.G., and R.M. All authors have read and agreed to the published version of the manuscript.

**Funding:** This research received no external funding.

**Conflicts of Interest:** The authors declare no conflict of interest.

## References

1. Zhou, Y.-L.; Li, H.-W. The Analysis of Gas-Liquid Two-Phase Flow Patterns Based on Variation Coefficient of Image Connected Regions and Line-Correlation Algorithm. *Energy Procedia* **2012**, *17*, 933–938. [CrossRef]
2. Thome, J.R. Boiling in microchannels: A review of experiment and theory. *Int. J. Heat Fluid Flow* **2004**, *25*, 128–139. [CrossRef]
3. Dupont, V.; Thome, J.R.; Jacobi, A.M. Heat transfer model for evaporation in microchannels. Part II: Comparison with the database. *Int. J. Heat Mass Transf.* **2004**, *47*, 3387–3401. [CrossRef]
4. Kandlikar, S.G. Fundamental issues related to flow boiling in minichannels and microchannels. *Exp. Therm. Fluid Sci.* **2002**, *26*, 389–407. [CrossRef]
5. Grzybowski, H.; Mosdorf, R. Dynamics of pressure drop oscillations during flow boiling inside minichannel. *Int. J. Heat Mass Transf.* **2018**, *95*, 25–32. [CrossRef]
6. Qu, W.; Yoon, S.-M.; Mudawar, I. Two-Phase Flow and Heat Transfer in Rectangular Micro-Channels. In *Heat Transfer*; ASME: Las Vegas, NV, USA, 2003; pp. 397–410.
7. Pei, L.; Kuang, J.; Shao, Y. The frequency characteristic of chaotic synchronization systems and weak signal detection. *Sci. China Ser. E-Technol. Sci.* **1997**, *40*, 472–478. [CrossRef]
8. Górski, G.; Litak, G.; Mosdorf, R.; Rysak, A. Dynamics of a two-phase flow through a minichannel: Transition from churn to slug flow. *Eur. Phys. J. Plus.* **2016**, *131*, 111. [CrossRef]
9. Litak, G.; Górski, G.; Mosdorf, R.; Rysak, A. Study of dynamics of two-phase flow through a minichannel by means of recurrences. *Mech. Syst. Signal Process.* **2017**, *89*, 48–57. [CrossRef]
10. Rysak, A. Dynamics of two-phase flow analyzed by multi-gate correlations. *Exp. Therm. Fluid Sci.* **2018**, *98*, 397–405. [CrossRef]
11. Mastrullo, R.; Mauro, A.W. Peripheral Heat Transfer Coefficient during Flow Boiling: Comparison between 2-D and 1-D Data Reduction and Discussion about Their Applicability. *Energies* **2019**, *12*, 4483. [CrossRef]
12. Ibrahim-Rassoul, N.; Si-Ahmed, E.-K.; Serir, A.; Kessi, A.; Legrand, J.; Djilali, N. Investigation of Two-Phase Flow in a Hydrophobic Fuel-Cell Micro-Channel. *Energies* **2019**, *12*, 2061. [CrossRef]
13. Kashdan, J.T.; Shrimpton, J.S.; Whybrew, A. Two-Phase Flow Characterization by Automated Digital Image Analysis. Part 1: Fundamental Principles and Calibration of the Technique. *Part. Part. Syst. Charact.* **2003**, *20*, 387–397. [CrossRef]
14. Masiukiewicz, M.; Anweiler, S. Two-phase flow phenomena assessment in minichannels for compact heat exchangers using image analysis methods. *Energy Convers. Manag.* **2015**, *104*, 44–54. [CrossRef]
15. Do Amaral, C.E.F.; Alves, R.F.; da Silva, M.J.; Arruda, L.V.R.; Dorini, L.; Morales, R.E.M.; Pipa, D.R. Image processing techniques for high-speed videometry in horizontal two-phase slug flows. *Flow Meas. Instrum.* **2013**, *33*, 257–264. [CrossRef]
16. Mosdorf, R.; Grzybowski, H.; Gruszczyńska, I. Modelling of non-stationary pressure fluctuations during boiling in a minichannel. *Proc. E3S Web Conf.* **2019**, *128*, 04007. [CrossRef]
17. Park, I.W.; Fernandino, M.; Dorao, C.A. On the occurrence of superimposed density wave oscillations on pressure drop oscillations and the influence of a compressible volume. *AIP Adv.* **2018**, *8*, 075022. [CrossRef]